Measurement of Apparent Thermal Conductivity of Multilayer Insulations at Low-Compressive Loads

VERNON L. HOLMES* AND LEON E. MCCRARY†
McDonnell Aircraft Company, St. Louis, Mo.
AND
DENNIS R. KRAUSE‡
McDonnell Douglas Astronautics Company, Huntington Beach, Calif.

Four multilayer insulations, selected for potential applications on future multimission space vehicles, have been evaluated. The effective thermal conductivities of the insulations were determined at a minimum of four compressive loads between 10^{-4} and 10^{-1} psi. The equivalent thermal conductivity of one of the test specimens was determined at two compressive loads with interstitial helium gas pressure of 10^{-3} and 1.0 torr. Particular attention was given to techniques for minimizing errors in obtaining thermal conductivity data. Double Goldized Kapton/Dacron B4A composite, displayed the lowest thermal conductivity and $k\rho$ product of the four composites evaluated at compressive loads below 10^{-2} psi. Thermal conductivity of the multilayer insulations tested was insensitive to small changes in mechanical loading at 1.0 torr interstitial gas pressure, but became increasingly more sensitive to mechanical loading as the interstitial gas pressure was reduced.

Introduction

MULTILAYER insulations offer insulating qualities superior to those of fibrous materials, powders, or foams for in-space applications, and since multilayer insulations also have the lowest thermal conductivity-density product ($k\rho$) of these classes of insulations, their use on space vehicles not only provides the best possible thermal protection but also effects substantial weight savings.

The next generation of space vehicles will include multilaunch vehicles. This will result in multilayer insulations being subjected to numerous compressive and expansive loading forces due to evacuation, repressurization, and acceleration. Inasmuch as the thermal performance of the insulation is affected by its layer density, data concerning the performance of candidate multilayer insulations at various layer densities are needed for material selection and system design.

The effective thermal conductivity of four high performance insulations (HPI) was determined by calorimetry at a minimum of four compressive loads (4 layer densities) between 10^{-4} and 10^{-1} psi. The pressure within the calorimeter was less than 10^{-6} torr for each of the four insulation tests. In addition, the equivalent thermal conductivity of one of the test specimens was determined at two compressive loads and with interstitial gas pressures of 10^{-3} and 1.0 torr. In all tests the cold face temperature of the insulation was maintained at $-320°F$ with the warm side of the test specimen at approximately room temperature.

Test Specimens

The HPI specimens were composed of ten layers of reflector/separator pairs. The particular composite reflector/separator pairs evaluated were Double Aluminized Kapton (DAK)/Nomex HT-287, Double Goldized Kapton (DGK)/Nomex HT-287, DGK/Nomex HT-96 and DGK/Dacron B4A. The specimens were 20.4 in. in diam with thicknesses between 0.227 and 0.135 in. A typical specimen is shown in Fig. 1.

All specimens were handled with gloves to prevent contamination of the low emissivity surfaces of the reflectors. The specimens were cut using a template having an inner diameter of 20.4 in. and having tabs for fastening the layer-pairs together. Fastening the layers together at the tabs prevented slippage of the layer-pairs before installation in the test calorimeter. Compression of the insulation during installation in the calorimeter was minimized by exercising extreme care and by handling only the tabs which were external to the test area of the specimen.

Test Setup and Instrumentation

A double guarded flat-plate calorimeter, utilizing the boil-off of a cryogenic liquid to measure the heat flux through the insulations, was used to determine the effective thermal conductivity of the composites. In these tests, liquid nitrogen was used to obtain a cold face temperature of $-320°F$.

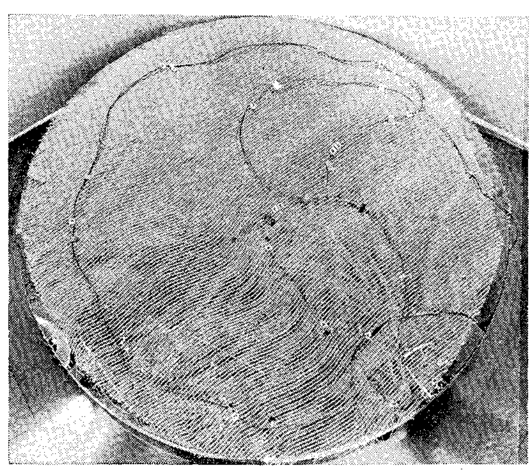

Fig. 1 Typical thermal conductivity specimen (Double Goldized Kapton (DGK)/Nomex HT-96).

Presented as Paper 72-367 at the AIAA/ASME/SAE 13th Structures, Structural Dynamics, and Materials Conference, San Antonio, Texas, April 10–12, 1972; submitted April 17, 1972, revision received June 26, 1972. This work is related to NASA Contract NAS 8-26006.

Index categories: Spacecraft Temperature Control Systems; Radiation and Radiative Heat Transfer.

* Test Engineer.
† Senior Group Engineer.
‡ Engineering Scientist Specialist.

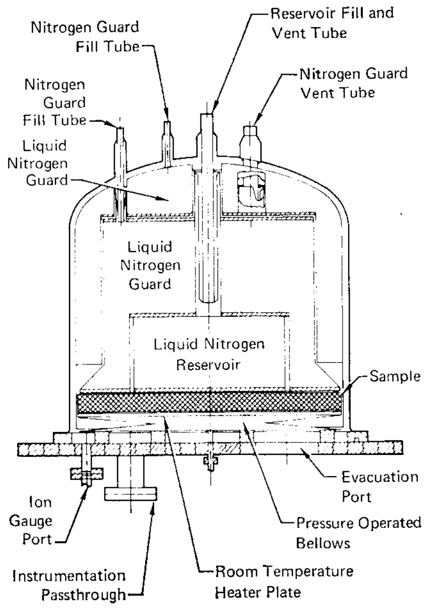

Fig. 2 Flat plate calorimeter.

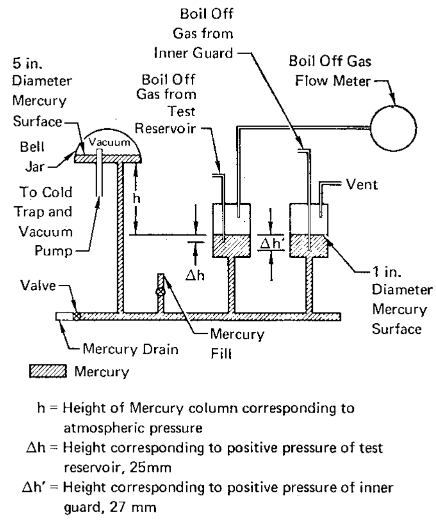

Fig. 3 Calorimeter gas-pressure control system.

The calorimeter, shown schematically in Fig. 2, consists of a 12-in.-diam central test reservoir surrounded by two guard reservoirs. A 4-in.-wide inner guard surrounds the central test reservoir and the outer guard surrounds both inner reservoirs. Both guards were filled with the same cryogen (LN_2) that was in the central test reservoir.

A copper curtain, attached to the outer guard, extends down past the inner guard and past the specimen. This curtain, cooled by conduction from the outer guard, establishes a cold wall for radiation exchange between the outer edge of the specimen and the calorimeter. This results in a significant reduction in lateral heat transfer in the specimen, improvement of one-dimensional heat transfer normal to the specimen under steady state conditions, and an increase in the accuracy of the data.

The hot-face side of the specimen was controlled at ambient temperature by a 20.5-in.-diam specimen heater. A 0.5-in.-thick aluminum plate was used between the specimen heater and the insulation composite to reduce any local power density variations from the wire-wound heater; this prevented local hot spots.

Because high-performance insulations require a long time to establish steady-state heat transfer for small heat fluxes, disturbance of the cryogen in the calorimeter must be minimized. Variations in the temperature of the liquid nitrogen are caused by atmospheric pressure changes, by refilling of the reservoir with cryogenic fluid, and by rapid boiloff of the cryogenic liquid, all of which were minimized in this test. The outer guard reduced the heat leak into the inner guard sufficiently to permit tests at all compressive loads to be evaluated without the need for refilling the inner guard or the' test reservoir.

The detrimental effects of temperature and boiloff variations for liquid nitrogen within the calorimeter, caused by changes in atmospheric pressure, were reduced by a factor of 25 by using the gas pressure control system shown schematically in Fig. 3 and described in detail in Ref. 1.

The amount of the inherent heat leak into the central reservoir was measured at the test pressure and temperature used in the subsequent tests on the composite specimens. The heat leak determination was made by adding a cold plate between the test reservoir and the bellows pressurization system to reduce radiation to the central reservoir. The plate was cooled to approximately liquid nitrogen temperature (average temperature of $-304°F$) to reduce heat exchange between the test reservoir and the coldplate. During the inherent heat leak test, the pressure in the calorimeter was maintained at less than 5×10^{-6} torr.

For the thermal conductivity tests, the specimens were loaded mechanically by the use of a pressure-operated bellows placed under the heater. The bellows pressure was measured by a Baratron[§] pressure gage.

The thickness of the insulation, which was the distance between the reservoir (cold plate) and the hot plate, was measured indirectly at 10^{-3} torr, by recording the movement of the bellows on which the hot plate rested. A glass tube which contained a spring-loaded metal pointer that extended into and reacted against the top of the bellows was placed in the bellows pressurization line. Movement of the bellows and therefore compression of the sample was measured by determining the movement of the metal pointer with a cathetometer. A one-to-one correspondence was established between the bellows extension, measured external to the calorimeter with the cathetometer, and different reservoir-to-plate spacing. The change in the spacing was corrected for thermal contraction that occurred during the cool-down to liquid nitrogen temperature. The uncertainty of the cathetometer measurements was ± 0.002 in.

The total pressure applied to the bellows was not transmitted to the insulation as a compressive load. The total applied pressure instead produced extension of the bellows to the initial insulation thickness (zero load), overcame the spring constant of the bellows for a small pressure increase above zero load, and compressed the insulation. Although the bellows pressure corresponding to a given reservoir spacing was measured several times and was reproducible, it was difficult to separate frictional forces in the bellows from compressive forces on the insulation at the very low-compressive loads. Since the thickness measurements were reliable, the compressive load on the test specimen at each point was obtained by measuring the insulation thickness and utilizing the data obtained in the compression tests.

Heat flux through the specimen was measured using a wet test gas flowmeter, calibrated for nitrogen gas, to monitor the boiloff exhaust gases from the central reservoir. The cold nitrogen gas was passed through several feet of tubing to permit the gas to warm and then was bubbled through water to increase the moisture content.

To evaluate the composites at an interstitial helium gas pressure of 10^{-3} and 1.0 torr it was necessary to isolate the sample from the calorimeter. The entire calorimeter could

§ MKS Instruments Inc., Burlington, Mass.

not be backfilled with helium gas since the heat leak from the external walls of the calorimeter to the cryogen would have been unacceptable. In order to achieve the 10^{-3} and 1.0 torr interstitial gas pressures in the test specimen, the specimen was "bagged" by placing a 0.25 mil mylar sheet over the sample and sealing the mylar to the aluminum plate with RTV Silastic 140¶ adhesive.

The compression characteristics of the HPI composites were used in interpreting the calorimeter test data. These compression characteristics were determined on several different composite specimens for up to 100 compression cycles on an Instron tensile test machine.[2] The compression test specimens of interest for the thermal conductivity test were DAK/Dacron B4A, DAK/Nomex HT-287, and DAK/Nomex HT-96. Two specimens, 15 × 15 in. and containing 10 layer pairs, were evaluated for each composite type. DAK reflector materials were used in all of the tests. Since the metal is only approximately 300–400 Å thick on the surface of the Kapton, the DAK data obtained in these tests were used for composites using DGK, assuming both to be the same in thickness.

Test Procedure

The 10 layer-pair specimens (10 reflectors and 10 separators) were placed in the calorimeter so that a separator was in contact with the cold plate and a reflector was in contact with the hot plate. The thermal conductivity as a function of compressive load was established by evaluating the insulation at successively increasing loads. At each successive step, the pressure applied to the bellows was held constant until steady-state heat transfer through the specimen was established. Steady-state heat transfer was reached when the boiloff rate of the liquid nitrogen became constant. Pressure in the calorimeter during the high vacuum tests was less than 10^{-6} torr for all four composites.

All of the tests using the Instron universal test machine to obtain layer-density vs compressive-load on the insulation were conducted in air at room temperature. A test fixture consisting of upper and lower platens with flat square faces (15 × 15 in.) was installed in the Instron machine, and the specimen was placed between these platens. Prior to testing, the upper platen was positioned above the lower platen at a distance equal to the free lay-up thickness of the specimen. This established a no-load reference position for the load cycle. The reading on a dial gage that monitored the displacement of the upper platen was taken at this no-load position. The platen position, as indicated by the dial gage, was also recorded at the maximum load position of the platen. These two readings of the dial gage were used to determine an accurate deflection scale for use in reading the data trace. The controls of the Instron were set so that the machine automatically cycled between the no-load machine setting and the maximum test load at a head speed of 0.2 in./min. Data reduction was not attempted below a load of

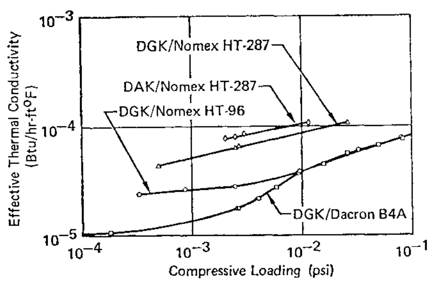

Fig. 4 Effective thermal conductivity-flat plate calorimeter data.

¶ Dow Corning Corp., Midland, Mich.

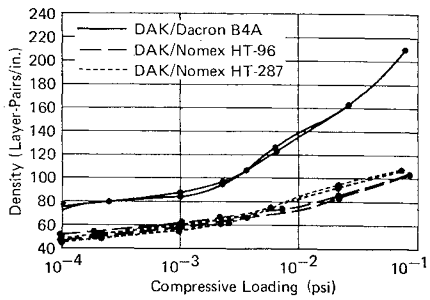

Fig. 5 Compressive characteristics of test specimens.

approximately 1×10^{-4} psi due to the minimal slope of the curve at lower compressive loadings. The uncertainty in reading the data from the curves at 1×10^{-4} psi was less than 2%.

The effective thermal conductivity of DGK/Dacron B4A composite at 10^{-3} and 1.0 torr interstitial helium pressure was evaluated in the same calorimeter using a similar procedure. First, the heat flux through the bagged specimen was determined at the minimum pressure obtainable in the bag ($<10^{-3}$ torr). Then, the heat flux through the bagged specimen was obtained at 10^{-4} and 10^{-3} psi compressive loads at 10^{-3} and 1.0 torr helium interstitial pressures, respectively. The layer densities required to produce the compressive loads were determined from the layer density vs compressive load curve for the 10 layer-pair composite specimen. Cyclic loading of the specimen was found to produce similar layer density vs compressive load curves, except for a shift due to permanent deformation. Before using the layer density vs compressive load curve to obtain the layer density corresponding to the desired compressive loads, the curve was shifted to correct for a zero shift caused by deformation of the specimen during the first evaluation of the DGK/Dacron B4A specimen.

Results and Discussion

The experimentally determined effective thermal conductivity (k) for each of the composites tested is shown in Fig. 4 and Tables 1-4.

The effects of interstitial helium gas pressure on the effective thermal conductivity of DGK/Dacron B4A under two loading conditions, 10^{-4} psi and 10^{-3} psi, and for two pressures 10^{-3} torr and 1.0 torr, are evident in the data of Table 5. The relationship of compressive loading and layer density of the insulation is presented in Fig. 5.

A comparison of the composite weights required to provide equivalent thermal performance, the $k\rho$ product, is used for ranking purposes. The $k\rho$ values obtained from the calorimeter test data are shown in Fig. 6 and Tables 1-4. The Dacron B4A separator clearly provides the lowest system weight and, therefore, best thermal performance of

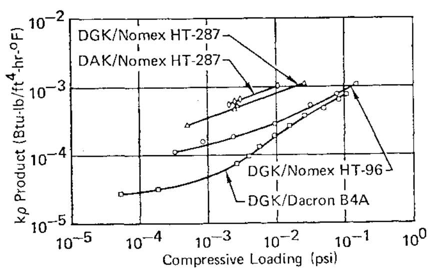

Fig. 6 Thermal performance ($k\rho$) of multilayer insulations.

Table 1 DAK/Nomex HT-287 flat plate calorimeter data

Layer Density (Layer pairs/inch)	Net Heat Rate		Insulation Thickness		Effective Thermal Conductivity (k)		Compressive Load (psi)	Weight Density (lb/ft³)	kρ (Btu-lb/ft⁴-Hr-°F)
	Btu/ Hr	Cal/ Sec	(Inches)	(Cm)	Btu/ Ft-Hr-°F	Cal/ Cm-Sec-°C			
64.1	1.84	0.129	0.150	0.380	7.2×10^{-5}	3.0×10^{-7}	2.1×10^{-3}	7.46	5.6×10^{-4}
65.4	2.03	0.142	0.146	0.370	7.7×10^{-5}	3.2×10^{-7}	2.5×10^{-3}	7.60	6.2×10^{-4}
67.1	2.26	0.158	0.139	0.352	8.2×10^{-5}	3.4×10^{-7}	3.0×10^{-3}	7.81	6.7×10^{-4}
84.0	3.44	0.241	0.110	0.279	9.9×10^{-5}	4.1×10^{-7}	1.2×10^{-2}	9.78	1.0×10^{-3}

Table 2 DGK/Nomex HT-287 flat plate calorimeter data

Layer Density (Layer pairs/inch)	Net Heat Rate		Insulation Thickness		Effective Thermal Conductivity (k)		Compressive Load (psi)	Weight Density (lb/ft³)	kρ (Btu-lb/ft⁴-Hr-°F)
	Btu/ Hr	Cal/ Sec	(Inches)	(Cm)	Btu/ Ft-Hr-°F	Cal/ Cm-Sec-°C			
55.2	0.900	0.063	0.181	0.459	4.2×10^{-5}	1.7×10^{-7}	5.0×10^{-4}	6.42	2.7×10^{-4}
65.4	1.60	0.112	0.153	0.389	6.3×10^{-5}	2.6×10^{-7}	2.5×10^{-3}	7.60	4.8×10^{-4}
66.2	1.71	0.120	0.151	0.384	6.7×10^{-5}	2.8×10^{-7}	2.7×10^{-3}	7.70	5.1×10^{-4}
92.6	3.80	0.266	0.108	0.274	1.1×10^{-4}	4.4×10^{-7}	2.6×10^{-2}	11.78	1.2×10^{-3}

Table 3 DGK/Nomex HT-96 flat plate calorimeter data

Layer Density (Layer pairs/inch)	Net Heat Rate		Insulation Thickness		Effective Thermal Conductivity (k)		Compressive Load (psi)	Weight Density (lb/ft³)	kρ (Btu-lb/ft⁴-Hr-°F)
	Btu/ Hr	Cal/ Sec	(Inches)	(Cm)	Btu/ Ft-Hr-°F	Cal/ Cm-Sec-°C			
54.9	0.500	0.035	0.182	0.462	2.4×10^{-5}	9.8×10^{-8}	3.3×10^{-4}	5.46	1.3×10^{-4}
59.5	0.614	0.043	0.168	0.427	2.7×10^{-5}	1.1×10^{-7}	8.6×10^{-4}	5.93	1.6×10^{-4}
65.0	0.700	0.049	0.154	0.391	2.8×10^{-5}	1.2×10^{-7}	2.5×10^{-3}	6.48	1.8×10^{-4}
74.7	1.10	0.077	0.134	0.340	3.8×10^{-5}	1.6×10^{-7}	9.7×10^{-3}	7.43	2.8×10^{-4}
87.0	2.03	0.142	0.115	0.292	6.0×10^{-5}	2.5×10^{-7}	3.3×10^{-2}	8.66	5.2×10^{-4}
101.0	3.09	0.216	0.099	0.251	7.9×10^{-5}	3.3×10^{-7}	7.9×10^{-2}	10.08	8.0×10^{-4}
118.0	4.33	0.303	0.085	0.216	9.5×10^{-5}	3.9×10^{-7}	1.5×10^{-1}	11.70	1.1×10^{-3}
126.5	5.09	0.356	0.079	0.201	1.0×10^{-4}	4.3×10^{-7}		12.60	1.3×10^{-3}

Table 4 DGK/Dacron B4A flat plate calorimeter data

Layer Density (Layer pairs/inch)	Net Heat Rate		Insulation Thickness		Effective Thermal Conductivity (k)		Compressive Load (psi)	Weight Density (lb/ft³)	kρ (Btu-lb/ft⁴-Hr-°F)
	Btu/ Hr	Cal/ Sec	(Inches)	(Cm)	Btu/ Ft-Hr-°F	Cal/ Cm-Sec-°C			
65.8	0.257	0.018	0.152	0.386	1.0×10^{-5}	4.2×10^{-8}	4.6×10^{-5}	2.61	2.7×10^{-5}
78.2	0.314	0.022	0.128	0.325	1.0×10^{-5}	$4.3 - 10^{-8}$	1.8×10^{-4}	3.09	3.2×10^{-5}
103.1	0.700	0.049	0.097	0.246	1.8×10^{-5}	7.3×10^{-8}	2.6×10^{-3}	4.08	7.2×10^{-5}
113.7	0.929	0.065	0.088	0.224	2.1×10^{-5}	8.8×10^{-8}	4.0×10^{-3}	4.49	9.5×10^{-5}
123.5	1.29	0.090	0.081	0.206	2.7×10^{-5}	1.1×10^{-7}	5.8×10^{-3}	4.88	1.3×10^{-4}
137.0	1.87	0.131	0.073	0.185	3.5×10^{-5}	1.5×10^{-7}	9.2×10^{-3}	5.41	1.9×10^{-4}
151.5	2.59	0.181	0.066	0.168	4.4×10^{-5}	1.8×10^{-7}	1.6×10^{-2}	6.00	2.7×10^{-4}
164.0	3.63	0.254	0.061	0.155	5.7×10^{-5}	2.4×10^{-7}	2.6×10^{-2}	6.49	3.7×10^{-4}
185.0	4.86	0.340	0.054	0.137	6.7×10^{-5}	2.8×10^{-7}	5.0×10^{-2}	7.33	4.9×10^{-4}
208.5	6.14	0.430	0.048	0.122	7.6×10^{-5}	3.1×10^{-7}	8.2×10^{-2}	8.25	6.2×10^{-4}
232.5	7.70	0.539	0.043	0.109	8.5×10^{-5}	3.5×10^{-7}	1.2×10^{-1}	9.20	7.8×10^{-4}

Table 5 Thermal conductivity of DGK/Dacron B4A vs interstitial helium gas pressure and compressive load

Interstitial He Gas Pressure (torr)	Net Heat Rate		Insulation Thickness		Effective Thermal Conductivity		Compressive Load (psi)
	(Btu/Hr)	(Cal/Sec)	(Inches)	(Cm)	Btu/ Ft-Hr-°F	Cal/ Cm-Sec-°C	
$<1.0 \times 10^{-3}$	1.04	0.073	0.105	0.267	2.8×10^{-5}	1.2×10^{-7}	1.0×10^{-4}
1.0×10^{-3}	1.51	0.106	0.105	0.267	4.0×10^{-5}	1.7×10^{-7}	1.0×10^{-4}
1.0	40.29	2.820	0.105	0.267	1.2×10^{-3}	5.0×10^{-6}	1.0×10^{-4}
1.0×10^{-3}	7.11	0.498	0.085	0.216	1.7×10^{-4}	7.2×10^{-7}	1.0×10^{-3}
1.0	49.74	3.482	0.085	0.216	1.2×10^{-3}	5.0×10^{-6}	1.0×10^{-3}

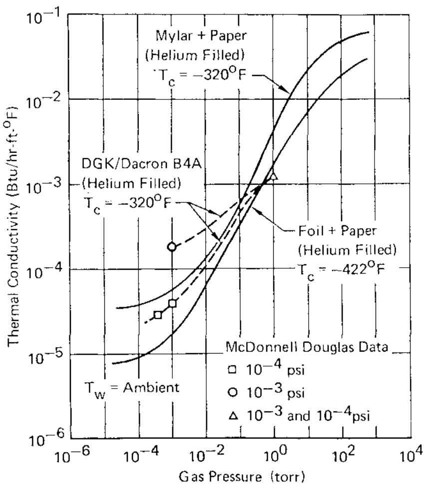

Fig. 7 Thermal conductivity of multilayer composites as a function of gas pressure and loading.

the three separators tested. The DGK/Nomex HT-96 has a lower $k\rho$ product than the DGK/Nomex HT-287 but a significantly higher one than the DGK/Dacron B4A at the compressive loads of primary interest ($<10^{-3}$ psi). A good correlation exists between these results and those for similar test specimens.[3] These data are compared in Fig. 7.

Conclusions

During this program it was determined that 1) the DGK/Dacron B4A composite provides the lowest thermal conductivity and $k\rho$ product of the four composites evaluated for compressive loads less than 10^{-2} psi. 2) The Nomex HT-96 has a lower $k\rho$ product than the Nomex HT-287, but a significantly higher one than the Dacron B4A at low-compressive loads. 3) The composite insulation utilizing the goldized reflector has a slightly lower effective thermal conductivity than the aluminized reflector when used with the Nomex HT-287 separator. 4) The thermal conductivity of DGK/Dacron B4A at 10^{-4} psi compressive load and 10^{-3} torr pressure is 4.0×10^{-5} BTU/Ft-Hr-°F which is four times the value at a similar compressive load and 10^{-6} torr. The value at 10^{-4} psi and 1.0 torr is 120 times the value at the same compressive load and 10^{-6} torr. 5) The thermal conductivity of DGK/Dacron B4A at 10^{-3} psi compressive load and 10^{-3} torr is 1.7×10^{-4} BTU/Ft-Hr-°F which is 12 times the value at 10^{-3} psi and 10^{-6} torr. 6) The thermal conductivity of DGK/Dacron B4A is insensitive to a change in compressive loading from 10^{-4} to 10^{-3} psi at 1.0 torr helium interstitial gas pressure. 7) The thermal conductivity of the multilayer insulations is insensitive to small changes in mechanical loading at 1.0 torr interstitial gas pressure, but becomes increasingly more sensitive to mechanical loading as the interstitial gas pressure is reduced.

References

[1] Black, I. A. and Glaser, P. E., *Advances in Cryogenic Engineering*, Vol. 9, Plenum Press, New York, 1964, p. 52.

[2] Krause, D. R., "Development of Lightweight Material Composites to Insulate Cryogenic Storage Tanks for 30-Day Storage in Outer Space," MDC G2348, Fourth Quarterly Report, NASA Contract NAS 8-26006, June 1971, McDonnell Douglas Corp., Huntington Beach, Calif.

[3] Parmley, R. T., "Handbook of Thermal Design Data for Multilayer Insulation Systems," LMSC-A742593-VI, NASA Contract NAS 8-11347, Aug. 1965, Lockheed Corp., Sunnyvale, Calif.